KICSP 한국 융합신호처리학회

융합신호처리학회논문지 Vol. 23, No. 2 : 50~61 June. 2022
DOI : 10.23087/jkicsp.2022.23.2.001

Aqua-Aware: Underwater Optical Wirelesss Communication enabled Compact Sensor Node, Temperature and Pressure Monitoring for Small Moblie Platforms

Maaz Salman[1], Javad Balboli[1], Ramavath Prasad Naik[1], Wan-Young Chung[2*],Jong-Jin Kim[2*]
[1]Department of Artificial Intelligence and Convergence, Pukyong national university
[2]Department of Electronic Engineering, Pukyong national university

Abstract This work demonstrates the design and evaluation of Aqua-Aware, a lightweight miniaturized light emitting diode (LED) based underwater compact sensor node which is used to obtain different characteristics of the underwater environment. Two optical sensor nodes have been designed, developed, and evaluated for a short and medium link range called as Aqua-Aware short range (AASR) and Aqua-Aware medium range (AAMR), respectively. The hardware and software implementation of proposed sensor node, algorithms, and trade-offs have been discussed in this paper. The underwater environment is emulated by introducing different turbulence effects such as air bubbles, waves and turbidity in a 4-m water tank. In clear water, the Aqua-Aware achieved a data rate of 0.2 Mbps at communication link up to 2-m. The Aqua-Aware was able to achieve 0.2 Mbps in a turbid water of 64 NTU in the presence of moderate water waves and air bubbles within the communication link range of 1.7-m. We have evaluated the luminous intensity, packet success rate and bit error rate performance of the proposed system obtained by varying the various medium characteristics.

• Key Words : Aqua-Aware, LED, AASR, AAMR, packet success rate, bit error rate.

Received 7 June 2022, Revised 25 June 2022, Accepted 27 June

* **Corresponding Author** Wan-Young Chung and Jong-Jin Kim, Department of Electronic Engineering, Pukyong national university, Busan, South Korea. E-mail: wychung@pknu.ac.kr, kimjj@pknu.ac.kr

Ⅰ. Introduction

Nowadays, wireless communication is utilized in wide areas of terrestrial applications[1]. However, underwater is still unexplored territory due to harsh and dynamic environment. Therefore, developing a wireless communication system for this environment plays a vital role. There are many applications that can benefit from the development of underwater wireless communication such as seafloor temperature monitoring to predict volcanic activities, marine animals' location, and orientation tracking by using IMU sensors, and underwater pollution monitoring. For these purposes some underwater communication systems are available. The most common one is acoustic communication as it extends the underwater communication to send data up to 10's of miles[2]. But acoustic signals are restricted for low data-rate, high latency, and multipath propagation due to its high susceptibility of degradation characteristics. These drawbacks limit using this communication system for an application that should be monitored in real-time like marine life monitoring[3]. Although, radio frequency communication provides a relative alternative, but due to high attenuation rate in underwater channel the link range is limited to meters[4]. Considering all of the mentioned challenges, optical wireless communication promises better alternative as it provides high data-rates, minimal latency, and moderate link range. Literature suggests that the optical source wavelengths within the range of 450-530nm are less susceptible to the attenuation effects[5-7].

To study the behavior of optical light in underwater communication many studies have been done [9] and [10]. These studies theoretically and experimentally analyzed and proved the reliability of underwater communication systems. In terms of network, UOWC can be deployed in an underwater sensor network for underwater monitoring [11]. In [12], an analog underwater communication system was introduced that utilizes infrared light to send some fish species biological information. In [13], an underwater sensor network is demonstrated for optical data mulling that the performance of the optical modem was low. The communication in this system is extended in [14] and is improved in terms of data rate, power consumption, and range. In [15], the performance of a UWOC system utilizing different modulations and employing different degenerate cases is analyzed. It is shown that the use of MIMO, diversity scheme, and a proper channel codes lead to a suitable technique to reach a reliable-high-speed UWOC system. In [16] Schil et al. miniaturized the size of the transceiver in the optical communication system using a light-emitting diode. Most of the previous works are focused on the utilization of bulky, complex and expensive components to achieve higher data rate and link range [17-22]. These optical systems utilized off-board computing unit to process, encode/decode or modulate/de-modulate the data to further enhance the system performance. These underwater wireless optical communication system are suitable for complex and heavy duty applications such as seafloor monitoring, large UAVs, submarine, and ocean monitoring [21], [23], [24]. Based on these facts, we have developed a compact lightweight underwater wireless optical communication enabled sensor node to accommodate mobile and un-tethered communication. Furthermore, compact pressure and temperature sensors are employed to monitor the underwater characteristics or characteristics of a targeted body. Hence, we have coined the name, "Aqua-Aware" for the proposed compact sensor node. Due to these characteristics of our proposed system, Aqua-Aware is suitable for variety of applications such as fish monitoring, small UAVs, fish robots, divers and other similar platforms. The main contributions of this paper are as follows.

- Design and development of the Aqua-Aware sensor node.

- Employment of the compact sensors to realize the characteristics of the underwater environment or targeted body.
- We have evaluated experimental performances, such as: Packet success rate and luminous intensity with respect to link range, turbidity and concentration of air bubble population.
- Bit error rate of the proposed system under the influence of on-off keying and Manchester coding scenarios are evaluated.

The remaining part of this paper is organized as follows. Section II describes about the system model. Experimental demonstration is presented in Section III. Results and corresponding discussions are provided in Section IV. Finally paper is concluded in Section V.

Table 1. Comparison between different Underwater wireless communication system [8].

Parameter	Acoustic	RF	Optical
Attenuation	0.1 - 4 dB/km	3.5 - 5 dB/m	0.39 dB/m(ocean) 11 dB/m(turbid)
Speed	1500 ms-1	2.3×108 ms-1	2.3×108 ms-1
Data Rate	Kbps	Mbps	Gbps
Latency	High	Moderate	Low
Distance	> 100Km	< 10m	10 – 150m
Bandwidth	1kHz - 100 kHz	MHz	150 Mhz
Frequency Band	10 – 15Khz	3–300Mhz	5x1014Hz
Transmissio n Power	10W	mW-W	mW-W

Ⅱ. SYSTEM MODEL

2.1 Aqua-Aware Hardware

Two types of compact sensor nodes have been developed to accommodate and analyze the performance with different specifications: the short range compact node, Aqua-Aware Short Range (AASR), and the medium range compact optical node, Aqua-Aware Medium Range (AAMR). The range of the system depends on the aperture-size of the plano-convex lens that is used to focus the optical beam in a certain direction. Therefore, the compactness of the system has a trade off with the link range of the optical system. The medium range optical sensor node is designed to operate at low power, with in the range of 1-2 meters, with an optical source of $\theta = 5^\circ$ half power angle. The short range node is designed to operate at low power, with in the range of 1 meters with an increased half power angle of $\theta = 120^\circ$. The field of view of both systems' receiver is fixed at $\phi = 0^\circ$ [30, 31]. The trade off is analyzed in term of performance, link range, and cost for both systems. The block diagram of both systems with the compact sensors are illustrated in Fig. 1.

2.1.1 Short Range Compact Sensor Node:

The Aqua-Aware Short Range is comprised of two main components, a compact optical sensor node which utilizes the optical communication to transmit the sensors data along the channel, an optical receiver which translates the modulated light intensity

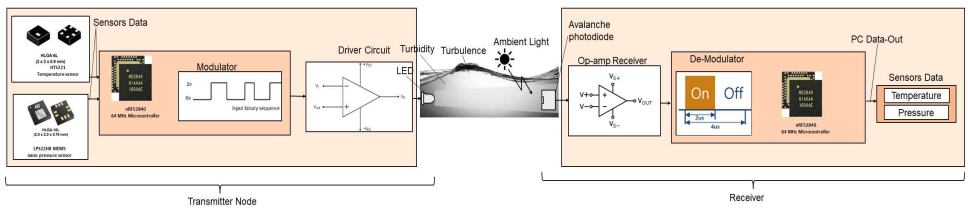

Fig. 1. Block diagram of the Compact Underwater Optical Wireless Communication System.

into stream of electrical pulses. The compact sensor node is 55×25×15 (mm)3. The system utilizes two sensors i.e. HTS221 and LPS22HB MEMS to compute temperature and pressure of a targeted body or environment, respectively. The micro-controller, Nordic-Semiconductor nRF52480 store this data in an array for further signal processing. The modulation algorithm, on-off keying and Manchester encoding, takes a byte of data from this array and converts into stream of binary data. The modulation algorithm transmit this data in the form of pulses with respect to their binary individual bit. The optical signal drives by the transmitter circuit, comprised of analog comparator (LM393) and NPN bipolar junction transistor (2N3904). The optical transmitter is used to switch and compare the electrical signal and form the corresponding optical pulses in stream of highs (5V) and lows (0V). The circuit diagram of optical transmitter is shown in 2. The receiver consists of Si-PIN photodiode (Hamamatsu S5107) which converts the optical pulses into electrical pulses. These stream of weak pulses are fed to the voltage follower buffer section (TL082) then amplified up to 100 times by the TL082 amplifier and the LM393 transistor chip uses these pulses for transistor to transistor logic comparison i.e. 0 or 5V. Furthermore, the receiver circuit utilizes LMC7660 IC to generate -5V to feed the buffer and amplifier. The circuit diagram of the receiver section is shown in 2. The digitized output from the TIA based optical receiver is decoded using the nRF52480 micro-controller into series of information bytes. Fig. 3(c) shows the prototype of AASR compact sensor node.

2.1.2 Medium Range Compact Sensor Node:

The design architecture of medium range compact sensor node (Aqua-Aware medium range) is similar to the architecture of Aqua-Aware short range with the addition of 4° spot lens (LEDIL FCA1207 IRIS) to enhance the communication range of the node.

2.2. Aqua-Aware Software

The software of Aqua-Aware consists of three sections: temperature and pressure moderator/computer, modulator and de- modulator. The temperature and pressure moderator and modulator is located on the micro-controller of transmitter section whereas the de-modulator and the decoder sections function on the nRF52840 micro-controller (MCU) at the receiver section. The temperature and pressure moderator/computer takes 256 instances of data from the sensors, HTS221 and LPS22HB MEMS, moderates them by averaging all the collected data and transfers the computed result to the modulator section for further processing. This process is iterated in a continuous loop to get the instantaneous sensor data from the targeted entity i.e., marines' body or environment. The modulator grabs a byte of data from the array which contains the instantaneous values of the temperature and pressure, converts it into binary data and activate the digital port of the MCU according to the respective bit. The MSB of each byte is processed first leading to the LSB. The duration of the pulse is generated using the delay in microseconds. The MCU outputs the digital pin "high" if the bit is 1, and "low" if the binary bit is 0 and so on. Two types of modulation is used to drive the optical signal: on-off keying and RZ-Manchester Coded-on-off keying [25]. The data frame consists of header byte (sensor node ID) followed by the temperature and pressure value. The stop byte is added at the end of the frame for synchronization. The fundamental difference between these two is that the single bit is represented by individual high/low state of the digital pin in case of on-off keying, whereas combination of high followed by low state and vice versa is utilizes to represents the individual bit for RZ-Manchester Coded-on-off keying. The LED turns ON during the half interval of individual pulse for each bit, which compensate the flickering problem of the LED for Manchester coding. Although, this provides greater security but the bandwidth gets halved as compared to on-off keying.

The de-modulator/decoder algorithm is also programmed on the nRF52840 MCU running on 48MHz CPU clock. The digitized input from the TIA based optical receiver triggers the de-modulator to initiate the decoding process. The MCU runs at 48MHz to synchronize with the transmitter node and identify the individual pulse correctly. After the identification of sensor node ID from the transmitter, the de-modulator decodes the temperature and pressure data by processing the received byte according to the algorithm. The algorithm identifies the MSB and shift it left. This process continues until the LSB of a byte is received. Finally, the MCU sends this information to the PC for visualization.

III. Experimental setup

The major components and parameters used in this evaluation of the proposed underwater optical wireless communication enabled compact sensor nodes are following:

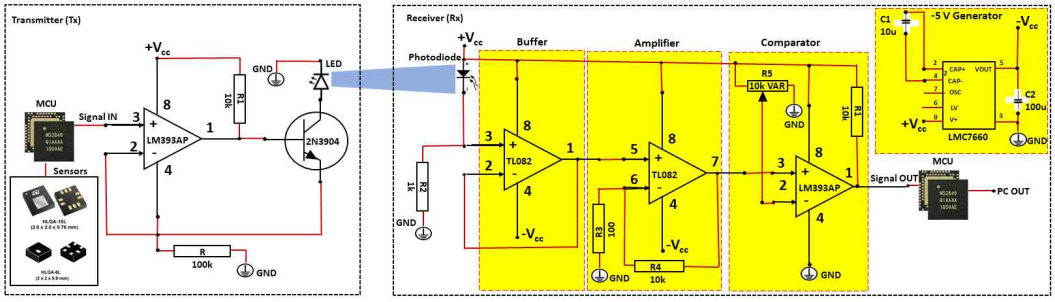

Fig. 2. Circuit diagram of the optical transmitter and receiver.

3.1 LED and Lens

The underwater optical wireless communication operating within the spectrum of 470-550nm faces minimum attenuation during the transmission of optical signal through clean or mildly turbid water (up to 70 NTU)[26]. Therefore, two LEDs, BIWV-PW5C5T and YINHUI HB10P-BLUE, of 470nm are employed in AAMR, and AASR, respectively, to drive the optical signal. The output power and maximum luminous intensity of both LEDs are 102 mW, and 2500 mcd, respectively.

Furthermore, 4° spot lens (LEDIL-FCA1207-IRIS) is employed in AAMR to enhance the communication range of the compact sensor node.

3.2 Photo-diode and Sensors

Both systems i.e. AAMR and AASR uses Si-PIN Photo-diode (S5107) of bandwidth 700-1050nm to realize the optical pulses and convert them into electrical attributes. The photosensitive area and peak sensitivity wavelength (λ_p) of the given photo-detector are $100\ mm^2$ and 960nm, respectively. The minimum response time of photo-detector is $1\mu s$. Compact temperature sensor (HTS221) of the size $2\times 22\times 0.9mm^3$, and pressure sensor (LPS22HB MEMS) of the size $2\times 2\times 0.76mm^3$ are employed on the compact sensor node to realize the environmental or physical parameters of the targeted entity.

3.3 Micro-controller

This work is focused on the compact size and dimensions of the sensor node to provide mobility and un-tethered communication for small mobile platforms such as fish monitoring, small underwater UAVs etc. Therefore, the nodes have been designed with the consideration of size constraints and the yielded complications and challenges. Therefore, a compact micro-controller nRF52840 from Nordic-Semiconductor

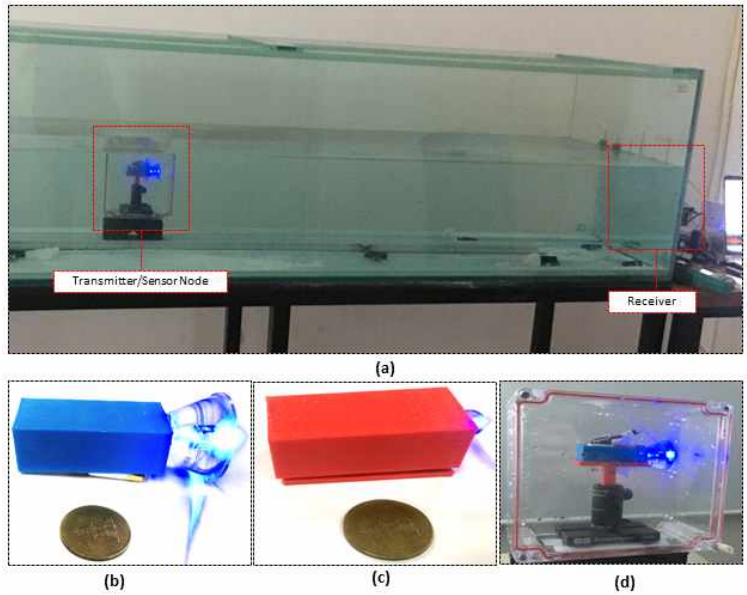

Fig. 3. Experimental setup and optical nodes. (a) Experimental setup. (b) Aqua-AwareMedium. (c) Aqua-AwareShort. (d) Water-tight Experiment box.

is employed to meet these requirements. The operating voltage of the MCU is 3.3Volts and is powered by compact 5V Li-Po battery to ensure the mobility requirement of the node.

3.4 Modulation

In this work, we have employed intensity modulated and directly detection (IMDD) schemes, such as return-to-zero (RZ)-on-off keying (OOK) and Manchester Coding modulation techniques. IMDD schemes are simple, easy to implement and less complex systems, hence using such modulation techniques gives faster and accurate responses. Hence, this technology is employed in both systems for faster and more accurate response, as well as to reduce the complexity, and size of the node. The RZ-on-off keying and Manchester Coding are utilized to transmit the optical signal along the water channel. The absence or presence of the pulse is identified as binary zero or one.

3.5 Underwater Channel

The real underwater environment comprises of many external disturbances which affect the transmission of optical signal through it. Water body has large amount of small hanging particles, concentration of small water bubbles, moving waves, and other minerals which absorb, deflect, diffract or attenuate the optical signal. This leads to absorption and scattering effects which results in the attenuation of the signal through the channel[27]. Therefore, artificial water waves are induced in the water tank of 4m by using a water pump with an airflow rate of 5 liters/min. Furthermore, small water bubbles are emulated by using an aerating jet of two outlets with the airflow rate of 1-2.5 liters/min. Different concentration of Zinc Oxide (ZnO) powder are added in the water to emulate the turbidity and small hanging particles in the natural body of water [28]. The turbidity of drinkable water is supposed to be 0.09 NTU whereas the ocean water turbidity should not exceed 50 NTU[29].

Table 2. Optical properties of water, namely, turbidity level (TU), transmittance (T), and absorbance (A) for different ZnO concentrations (C) [28].

Tu (NTU)	T (%)	A (m^{-1})	C (g/m^3)
0.9	89.1	5.00	0
0.36	88.4	5.41	16.78
1.71	87.0	6.01	33.57
25.42	85.3	7.00	67.14
64	81.0	9.01	117.49
70	80.3	9.61	142.67

The table 2 illustrated the relationship between the absorbance (A), turbidity level (TU), transmittance (T), and the concentration (C) of Zinc-Oxide powder[28]. The experimental parameters used in the evaluation for both systems are tabulated in table 3. Figure 3 (a) shows photographic illustration of the experimental setup used for the evaluation and demonstration of the system.

Table 3. Experimental parameters used in evaluation.

Transmitter	DC Power Battery		5V
	LED	Power (mW)	102
		Luminous Intensity (mcd)	2500
		Luminous Flux (lm)	1.5
		Wavelength (λ)	470
Channel	Aeration Jets	Airflow rate (l/min)	1-2.5
		Number of outlets	2
	Water pump (Displacement rate (l/min))		5
	Lighting Intensity (surroundings) (lux)		90.50
	Turbidity (NTU)		0-70
Receiver	Data Rate (Mbps)		0.2
	Si-PIN Photo-diode	Photosensitive Area (mm^2)	10×10
		Peak Sensitivity Wavelength (λ_p) (nm)	960

Ⅳ. Results and Discussions

In this section, we have presented various results, such as luminous intensity, packet success and bit error rates obtained from the experiment.

Fig. 4 shows the PSR and luminous intensity (lux) of short and medium ranges (AASR and AAMR) with respect to varying the link range. Fig. 4 represents PSR and luminous intensity plot for the AAMR, where the PSR and luminous intensity are reduces with the increase in link range at 64 NTU turbidity, and 1.5 L/min air bubble rate. Luminous intensity reduces from 6.9 lux to 5.7 lux with the increase in link range from 0.5-m to 2-m. Similarly, the percentage of packet successful rate decreases from 100 to 55 for the increase in link range from 0.5-m to 2-m. Similarly, Luminous intensity and PSR for the short range (AASR) is presented in Fig. 4b, where the 6.3 lux of luminous intensity and 100 percent PSR observed at 0.1-m link range, where as 5.7 lux luminous intensity and 50 percent PSR observed at 0.7-m of UWOC link range. Therefor, varying the link range from 0.1-m to 0.7-m causes 0.6 lux of luminous intensity degradation, which results 50 percent loss of packets. However, in medium link range (AAMR), varying the link range from 0.5-m to 2-m causes loss of 1.2 lux of luminous intensity, which results 45 percent of packet loss. Comparing the PSR results obtained by our proposed research with the research reported in [14], we can see the proposed AAMR obtains 60% PSR at 2.5-m link range in 64 NTU turbid water, whereas in [14], author's presented 60% PSR at 2.5-m link range with approximately 1 NTU turbid scenario. From these comparison, the research reported in this paper shows that the proposed setup can achieve same performance in heavy turbid scenarios.

success rate variation with respect to turbidity and air flow rate. In Fig. 5a, we have varied the turbidity level of the underwater medium from 0 to 70 Nephelometric turbidity units (NTU) and performed

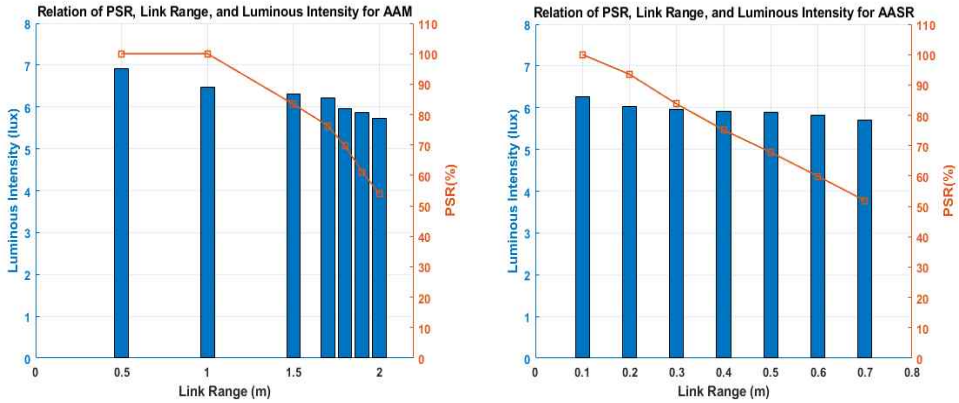

Fig. 4. Packet success rate and luminous intensity variation with respect to link range (a) AAMR (b) AASR

experiments at the air flow rate of 1.5 liters/min. Each time we have measured the successful packet received rate. A packet success rate of 76 percentage obtained for the distilled water (0 NTU turbidity) medium for the medium as well as short range links, where as the PSR obtained at 70 NTU turbidity are 62 percent in AAMR (1.7-m) and 39 percent in AASR (0.4-m) links, respectively. Similarly, the percentage of packet success rate for the varying air flow rates from 1 to 2.5 liters per minute underwater medium

minute airflow rate, respectively. An increased airflow rate from 1 to 2.5 liters per minute causes the degradation in the packet success rate to 53 and 49 percent for the AAMR and AASR links, respectively. From the Fig. 5, increase in the turbidity and airflow rate cause beam absorption and scattering effects, hence the packet success rate performance of the communication system deteriorates gradually.

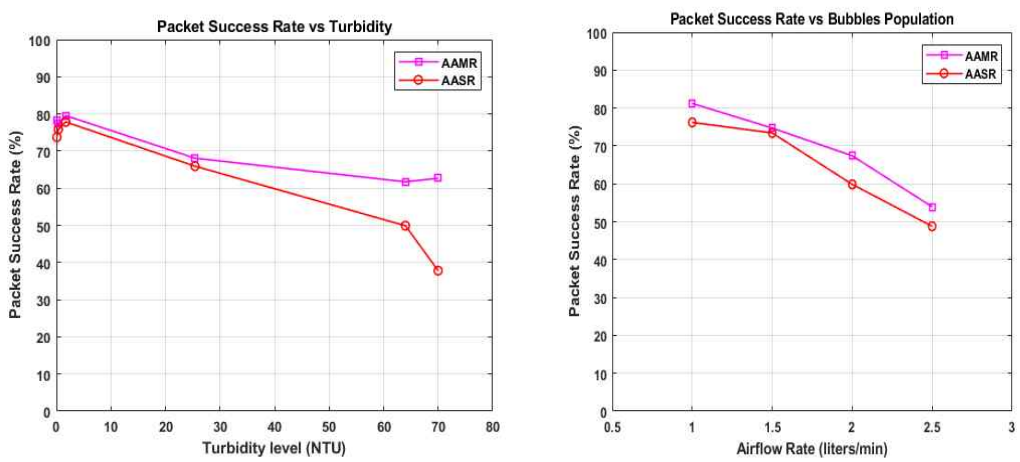

Fig. 5. Packet success rate variation (a) Turbidity levels and (b) Air bubble population Circuit diagram of the optical transmitter and receiver.

operated at the 64 NTU turbidity level is shown in Fig. 5b. Packet success rate of 81 and 77 percent obtained for AAMR and AASR links at 1 liters per

Fig. 6, shows the bit error rate of the AAMR link with respect to varying link range and signal to noise ratio. On-off keying and Manchester coding represents

the way of communication established in underwater scenarios. On-off keying transmits information bits such as 1 and 0 using the presence and absence optical beam, where as Manchester coding transmits 1 and 0 as optical beam presence for half duration-beam absence of half duration and beam absence of half duration-optical beam presence for half duration, respectively. Bit error rate represents the number of transmitted information bits are in error. In Fig. 6a, bit error rate performance of the system is obtained by varying the link range of the communication link for on-off keying and Manchester coding schemes.

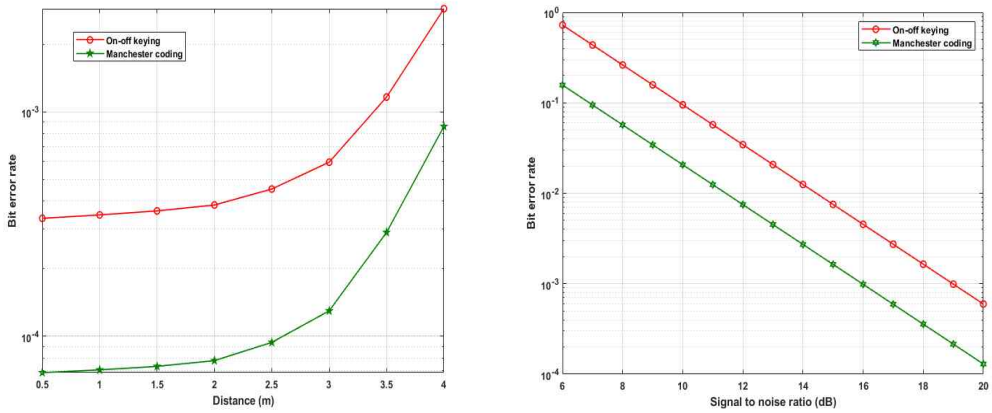

Fig. 6. Bit error rate variation (a) Distance, (b) Signal to noise ratio

Increase in the link range increases the bit error rate, which means increase in the number of errors. Comparing the bit error rate performance of on-off keying and Manchester coded modulation schemes, on-off keying modulation obtains 9×10^{-4} bit error rate at 3.3-m, whereas Manchester coded modulation obtains same bit error rate performance at 4-m link range. Hence, using the Manchester coding can increase 0.7-m link range over on-off keying modulation at 9×10^{-4} bit error rate. Similarly, the bit error rate performance obtained using the signal to noise ratio is shown in Fig. 6b, where signal to noise ratio indicates the ratio of received power to noise power for on-off keying as well as Manchester coding. Manchester coding performs 3 dB signal to noise ratio gain over the on-off keying at 1×10^{-3} bit error rate.

Fig. 7 shows temperature and pressure data collected from the experiment at 1.7-m AAMR link, 64 NTU turbidity, 1.5 liters per minute airflow rate. We have conducted experiment on May 25, 2022 at 10.30 AM, Busan. Maximum and minimum temperature are $22^\circ/16^\circ$, wind speed 45 Km/h and humidity 62% are weather details reported on May 25, 2022.

Maximum and minimum temperature and pressure data obtained from the experiment are $6^\circ/2^\circ$ and 80/200 pascals.

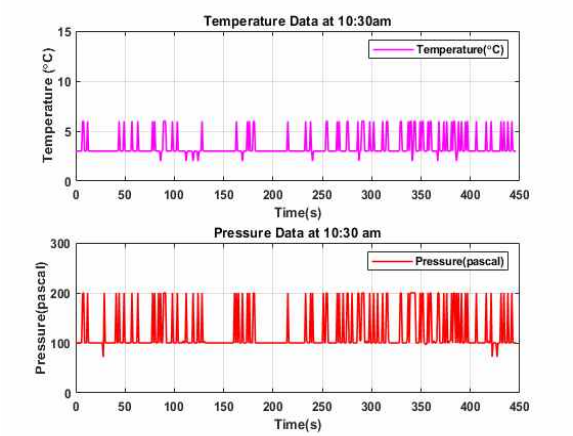

Fig. 7. Temperature and pressure data obtained from the experiment.

Ⅴ. Conclusion

In this paper, we have designed and developed Aqua-Aware underwater compact sensor node used for evaluating the underwater characteristics. Temperature and pressure data obtained from the underwater sensors are communicated via Aqua-Aware sensor node for the short and medium link ranges using AASR and AAMR, respectively. Luminous intensity, packet success rate and bit error rate performance of Aqua-Aware sensor node are evaluated experimentally. Packet success rate and luminous intensity fluctuations are obtained by varying the link ranges, turbidity level and airflow rate of the underwater medium. In addition to these results, we have evaluated bit error rate performance of the proposed system using on-off keying and Manchester coding schemes with respect to link range and signal to noise ratio. From the research reported in this paper, Aqua-Aware sensor nodes are efficient sensors to predict temperature as well as pressure metrics and then communicate them to the other nodes via UWOC links. In future works, some more parameters such as inertial moments, salinity and other underwater environmental characteristics and targeted marine body's parameters can also be evaluated using the proposed Aqua-Aware sensor nodes.

ACKNOWLEDGMENTS

This research work was supported by a Research Grant of Pukyong National University (2021).

REFERENCES

[1] M. A. S. Sejan and W.-Y. Chung, "Lightweight multi-hop vlc using compression and data-dependent multiple pulse modulation," Optics Express, vol. 28, no. 13, pp. 19 531–19 549, 2020.

[2] P. N. Ramavath, A. Kumar, S. Shashikant Godkhindi, and U. S. Acharya, "Experimental studies on the performance of underwater optical communication link with channel coding and interleaving," CSI Transactions on Ict, vol. 6, no. 1, pp. 65–70, 2018.

[3] R. Santos, J. Orozco, M. Micheletto, S. F. Ochoa, R. Meseguer, P. Millan, and C. Molina, "Real-time communication support for underwater acoustic sensor networks," Sensors, vol. 17, no. 7, p. 1629, 2017.

[4] S. Jiang and S. Georgakopoulos, "Electromagnetic wave propagation into fresh water," Journal of Electromagnetic Analysis and Applications, vol. 2011, 2011.

[5] P. N. Ramavath, S. A. Udupi, and P. Krishnan, "Co-operative rf-uwoc link performance over hyperbolic tangent log-normal distribution channel with pointing errors," Optics Communications, vol. 469, p. 125774, 2020.

[6] W.-Y. C. Maaz Salman, Javad Bolboli, "Experimental demonstration and evaluation of bch-assisted uwoc link for power efficient underwater sensor node," IEEE ACCESS, vol. XX, p. XXXX, 2022.

[7] P. N. Ramavath, S. A. Udupi, and P. Krishnan, "Experimental demonstration and analysis of underwater wireless optical communication link: Design, bch coded receiver diversity over the turbid and turbulent seawater channels," Microwave and Optical Technology Letters, vol. 62, no. 6, pp. 2207–2216, 2020.

[8] G. Schirripa Spagnolo, L. Cozzella, and F. Leccese, "Underwater optical wireless communications: Overview," Sensors, vol. 20, no. 8, p. 2261, 2020.

[9] F. Lu, S. Lee, J. Mounzer, and C. Schurgers, "Low-cost medium-range optical underwater modem: Short paper," in Proceedings of the Fourth ACM International Workshop on UnderWater Networks, 2009, pp. 1–4.

[10] B. Tu, L. Liu, Y. Liu, Y. Jin, and J. Tang, "Acquisition probability analysis of ultra-wide fov acquisition scheme in optical links under impact of atmospheric turbulence," Applied Optics, vol. 52, no. 14, pp. 3147–3155, 2013.

[11] C. Detweiller, I. Vasilescu, and D. Rus, "An underwater sensor network with dual communications, sensing, and mobility," in Oceans 2007-Europe. IEEE, 2007, pp. 1-6.

[12] Y. Tsuchida, N. Hama, and M. Takahata, "An optical telemetry system for underwater recording of electromyogram and neuronal activity from non-tethered crayfish," Journal of Neuroscience Methods, vol. 137, no. 1, pp. 103-109, 2004.

[13] I. Vasilescu, K. Kotay, D. Rus, M. Dunbabin, and P. Corke, "Data collection, storage, and retrieval with an underwater sensor network," in Proceedings of the 3rd international conference on Embedded networked sensor systems, 2005, pp. 154-165.

[14] M. Doniec, I. Vasilescu, M. Chitre, C. Detweiler, M. Hoffmann-Kuhnt, and D. Rus, "Aquaoptical: A lightweight device for high-rate long-range underwater point-to-point communication," in OCEANS 2009. IEEE, 2009, pp. 1-6.

[15] P. N. Ramavath, S. A. Udupi, and P. Krishnan, "High-speed and reliable underwater wireless optical communication system using multiple-input multiple-output and channel coding techniques for iout applications," Optics Communications, vol. 461, p. 125229, 2020.

[16] F. Schill, U. R. Zimmer, and J. Trumpf, "Visible spectrum optical communication and distance sensing for underwater applications," in Proceedings of ACRA, vol. 2004. Citeseer, 2004, pp. 1-8.

[17] J. A. Simpson, B. L. Hughes, and J. F. Muth, "Smart transmitters and receivers for underwater free-space optical communication," IEEE Journal on selected areas in communications, vol. 30, no. 5, pp. 964-974, 2012.

[18] C. Pontbriand, N. Farr, J. Ware, J. Preisig, and H. Popenoe, "Diffuse high-bandwidth optical communications," in OCEANS 2008. IEEE, 2008, pp. 1-4.

[19] M. Doniec, I. Vasilescu, M. Chitre, C. Detweiler, M. Hoffmann-Kuhnt, and D. Rus, "Aquaoptical: A lightweight device for high-rate long-range underwater point-to-point communication," in OCEANS 2009. IEEE, 2009, pp. 1-6.

[20] N. Farr, A. Chave, L. Freitag, J. Preisig, S. White, D. Yoerger, and P. Titterton, "Optical modem technology for seafloor observatories," in Proceedings of OCEANS 2005 MTS/IEEE. IEEE, 2005, pp. 928-934.

[21] D. Anguita, D. Brizzolara, and G. Parodi, "Optical wireless communication for underwater wireless sensor networks: Hardware modules and circuits design and implementation," in OCEANS 2010 MTS/IEEE SEATTLE. IEEE, 2010, pp. 1-8.

[22] F. Akhoundi, J. A. Salehi, and A. Tashakori, "Cellular underwater wireless optical cdma network: Performance analysis and implementation concepts," IEEE Transactions on Communications, vol. 63, no. 3, pp. 882-891, 2015.

[23] X. Tang, R. Kumar, C. Sun, L. Zhang, Z. Chen, R. Jiang, H. Wang, and A. Zhang, "Towards underwater coherent optical wireless communications using a simplified detection scheme," Optics Express, vol. 29, no. 13, pp. 19 340-19 351, 2021.

[24] C. Wang, H.-Y. Yu, and Y.-J. Zhu, "A long distance underwater visible light communication system with single photon avalanche diode," IEEE Photonics Journal, vol. 8, no. 5, pp. 1-11, 2016.

[25] P. N. Ramavath and W.-Y. Chung, "Evaluation of reconfigurable intelligent surface-assisted underwater wireless optical communication system," Journal of Lightwave Technology, 2022.

[26] G. Gilbert, T. Stoner, and J. Jernigan, "Underwater experiments on the polarization, coherence, and scattering properties of a pulsed blue-green laser," in Underwater Photo Optics I, vol. 7. SPIE, 1966, pp. 8-14.

[27] K. Liu and Y. Liang, "Underwater image enhancement method based on adaptive attenuation-curve prior," Optics express, vol. 29, no. 7, pp. 10 321-10 345, 2021.

[28] K. Enhos, E. Demirors, D. Unal, and T. Melodia, "Software-defined visible light networking for bi-directional wireless communication across the air-water interface," in 2021 18th Annual IEEE International Conference on Sensing, Communication, and Networking (SECON). IEEE, 2021, pp. 1-9.

[29] A. S. Trebitz, J. C. Brazner, V. J. Brady, R. Axler, and D. K. Tanner, "Turbidity tolerances of great lakes coastal wetland fishes," North American Journal of Fisheries Management, vol. 27, no. 2, pp. 619-633, 2007.

[30] Doniec, Marek, Michael Angermann, and Daniela Rus. "An end-to-end signal strength model for underwater optical communications." IEEE Journal of Oceanic Engineering 38, no. 4 (2013): 743-757.

[31] Wang, Chao, Hong-Yi Yu, and Yi-Jun Zhu. "A long distance underwater visible light communication system with single photon avalanche diode." IEEE Photonics Journal 8, no. 5 (2016): 1-11.

저자소개

MAAZ SALMAN

2018년 : 파키스탄 공과대학교 전기통신정보공학부(공학 학사)
2020년 : 순천향대학교 전기전자공학부(공학 석사)
2020년~현재 : 부경대학교 인공지능융합학과 박사과정

관심분야: 수중 사물 인터넷, 수중 광무선 통신, 인공지능, 센서 네트워크.

Javad Bolboli

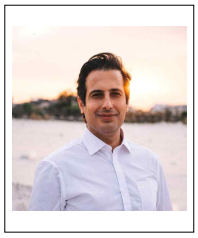

2013년 : 이란 마슈하드 SUT 대학교 전자공학부(공학 학사)
2017년 : Amirkabir University Technology, Tehran, Iran Control and Robotics Engineering(공학 석사)
2021년~현재 : 부경대학교 인공지능융합학과 박사과정

관심분야: Interner of things/Underwater Things, Underwater Optical Wireless Communication, Embedded Machine Learning and Artificial Intelligence

Ramavath Prasad Naik

2012년 : Jawaharlal Nehru Technology University, India 전기통신공학부(공학사)
2015년 : Motilal Nehru National Institute of Technology, India Allahabad, Uttar Pradesh 전기통신공학부(공학석사)
2021년 : National Institute of Engineering, Mysore 조교수
2021년 : National Institute of Engineering, Mysore 조교수
2021년~현재 : 부경대학교 Postdoctoral Researcher

관심분야: Free-Space and Underwater optical wireless communication, Theory and application of error control codes and Co-operative communication

정 완 영 (WAN-YOUNG CHUNG)

1987년 : 경북대학교 전자공학과(공학사)
1989년 : 경북대학교 전자공학과(공학석사)
1998년 : 큐슈대학교 센서공학(공학박사)
1999년~2008년 : 동서대학교 부교수
현재 : 부경대학교 전자공학과 정교수

관심분야: 무선 센서 네트워크, 유비쿼터스 의료 및 자동차 응용 프로그램, 가시광선 통신이 가능한 스마트 발광 시스템, 임베디드 시스템

김 종 진 (Jong-Jin Kim)

1983년 : 경북대학교 전자공학과(공학사)
1985년 : 한국과학기술원 전기및전자공학과(공학석사)
1995년 : 경북대학원 전자공학과(공학박사)
1987년~현재 : 부경대학교 전자컴퓨터정보통신공학부 정교수

관심분야: 컴퓨터구조, 컴퓨터네트워크, 컴퓨터 시스템응용